Acta Oceanol. Sin., 2017, Vol. 36, No. 9, P. 91–100
DOI: 10.1007/s13131-017-1114-z
http://www.hyxb.org.cn
E-mail: hyxbe@263.net

An available formula of the sandy beach state induced by plunging waves

JIANG Changbo[1, 2, 3], WU Zhiyuan[1, 2*], CHEN Jie[1, 2, 3], DENG Bin[1, 2, 3], LONG Yuannan[1, 2, 3], LI Lianjie[1]

[1] School of Hydraulic Engineering, Changsha University of Science and Technology, Changsha 410004, China

[2] Key Laboratory of Hunan Province for Water-sediment Sciences and Water Disaster Prevention, School of Hydraulic Engineering, Changsha University of Science and Technology, Changsha 410004, China

[3] International Research Center of Water Science and Environmental Engineering, Changsha University of Science and Technology, Changsha 410004, China

Received 14 June 2016; accepted 25 October 2016

Abstract

Laboratory experiments are performed to explore the response rule of a sandy beach profile under plunging wave on a non-uniform sediment-bed slope. The initial beach slope of combination of 1/10 and 1/20 is exposed to regular waves and cnoidal waves respectively. The free surface elevation, process of wave propagation, wave breaking, uprush and backwash and the change of a cross-shore beach profile are measured and recorded. The beach profile under the regular waves action exhibits two parts: a sandbar profile and a beach berm profile, and only one typical profile transformation under the cnoidal waves action is obtained, which is the beach berm profile. In the laboratory experiments, it is found that the beach states under wave action related to the previous factors. In addition, they are related to the characteristic of breaking waves such as the breaking intensity of the plunging wave. A concept about the characteristic angle of the plunging wave has been put forward through the observation and analysis of the phenomenon of the laboratory experiment. A qualitative analysis about the sediment transport carrying by currents generated from the plunging wave and the state of beach profile under the wave action has been done. The quantitative analysis about the relationship between the characteristic angle and Irribarren number has been done. An available formula of equilibrium states for the sandy beach induced by the plunging wave has been established based on the relationship between Irribarren number and the beach profile. By fitting these experimental results and others' experimental results to three lines, the three fitting coefficients can be calculated in their formula respectively. The recommended empirical formulas can divide three states of a beach morphology profile obviously, which include a depositive beach, an erosive beach and an intermediate beach.

Key words: formula of beach state, plunging wave, experimental study, regular wave, cnoidal wave

Citation: Jiang Changbo, Wu Zhiyuan, Chen Jie, Deng Bin, Long Yuannan, Li Lianjie. 2017. An available formula of the sandy beach state induced by plunging waves. Acta Oceanologica Sinica, 36(9): 91–100, doi: 10.1007/s13131-017-1114-z

1 Introduction

The morphology of the sandy beach depends mainly on coupling effects together with the contribution from wave, tide, flow and sediment. The cross-shore morphology of the sandy beach is an important issue for a coastal erosion (Grasso et al., 2009). Even though cross-shore sediment fluxes are usually a few orders of magnitude smaller than a longshore transport, the cross-shore beach profile has a strong influence on longshore velocity profiles and therefore on longshore sediment fluxes. The beach profile is the result of the trade-off between onshore and offshore fluxes. In addition, the intensity of the sediment transport during the uprush and the backwash is increased by the advection of turbulence and sediment from the surf zone due to bore collapse and/or wave breaking (Jackson et al., 2004; Pritchard and Hogg, 2005; Hughes et al., 2007; Alsina et al., 2009; Masselink et al., 2009). This complexity that the beach profile is normally dominate by the sediment transport in the surf zone with multiple wave breaks is very difficult to reproduce with numerical models and a physical model then becomes an interesting alternative.

Due to this complexity, the concept of equilibrium beach profile and its state formula are both very useful. In a stable wave field, the beach profiles will tend to be stable, and along with the wave and flow conditions change, the beach profile will change. From the 1940s, many scholars use coastal dynamics theory to expound beach profile states and a profile evolution rule through experimental study and field observation. Three types of the beach profile states had been classified as shown in Fig. 1, which include erosive beach, depositive beach and intermediate beach. The shoreline of the erosive beach is retreating, and the sediment sink down in an offshore zone to generate a sand bar, also known as sandbar profile. The shoreline of the depositive beach is advancing, and the sediment sinks down in a backshore zone to generate a berm, also known as a berm profile. The intermediate beach fall between the erosive beach and the depositive beach, and the sediment transport to two sides of the breaking point.

There is a beach profile classification which is based on the

Foundation item: The National Natural Science Foundation of China under contract Nos 51239001, 51179015, 51409022 and 51509023; the Hunan Provincial Innovation Foundation for Postgraduate under contract No. CX2015B348.
*Corresponding author, E-mail: stormsurge@126.com

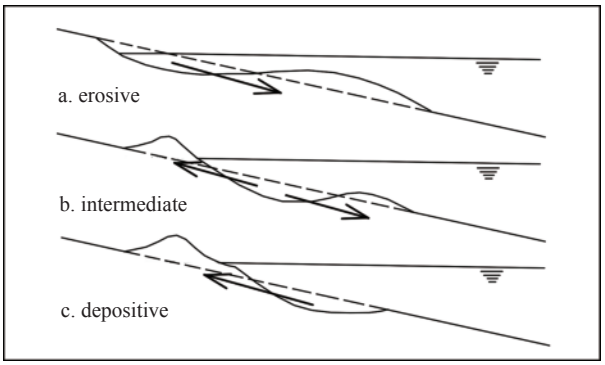

Fig. 1. Schematic types of beach profile state.

displacement of topography from the initial beach slope (Sunamura and Horikawa, 1974; Mimura et al., 1986) in Fig. 1. Type a indicates that a shoreline retrogresses and sediment accumulate in the offshore zone; Type b indicates that a shoreline progresses and no sediment deposition takes place offshore; and Type c indicates that a shoreline advances and sediment piles up offshore.

According to studying on the theory of the topography on Australia southeast coast, Wright and Thom (1977) first proposed six commonly occurring states and a coastal topographical dynamics theory, which had been known as the *Morphodynamics*. The six commonly occurring states were dissipative and reflective extremes and four intermediate states. There are many studies on a two-dimensional beach transformation and a cross-shore sediment transport in and out of the surf zone. Many investigations had been performed to determine parameters classifying beach profiles, such as by Johnson (1949), Dean(1973, 1991) and Xu (1988). A wave steepness, slope, and other nondimensional parameters had been adopted to their expressions respectively or concurrently.

The profile states of the beach erosion or deposition are influenced by sediment transport offshore and onshore directions, which controlled by some coastal dynamic factors, such as wave, current, sediment characteristics and other factors. The typical profile states of the sandy beach include ripple, sand bar, barrier and berm. Water waves were applied in a laboratory flume to investigate the evolutions of the velocity fields near a sandy bed. Many results obtained from an experimental investigation that were performed using irregular wave conducted to determine the wave-induced geometric characteristics of offshore ripples and bars were presented (Günaydın and Kabdaşlı, 2003b). The discussion of results from the laboratory experiments with regular wave sheds light on the gap that lies between the sediment transport associated with ripple migration and the performance of a standard bedload transport formula in terms of a bed shear concept (Yamaguchi and Sekiguchi, 2011). Laboratory data and large-scale laboratory data were presented on the influence of regular waves, irregular waves, free long waves, bound long waves, bichromatic wave groups and random waves on the sediment transport in the surf and swash zones (Doering and Baryla, 2002; Baldock et al., 2010, 2011; Tzang et al., 2011). In the experimental study, the regular wave, the random wave, the long wave, the wave group and the solitary wave (Roelvink et al., 1995; Reniers et al., 2001; Kobayashi and Lawrence, 2004; Baldock et al., 2010, 2011; Young et al., 2010; Alsina et al., 2012) were applied in a laboratory flume to investigate the evolutions on the sandy beach, and the rule of sediment transport and state of the beach profile had been researched. These studies were expected to reveal the relationship among types of wave, compose of sediment and state of sandy beach profile. These formulas (Bagnold, 1940; Sunamura and Horikawa, 1974; Guza and Inman, 1975; Kaneko, 1985; Günaydın and Kabdaslı, 2003a) mainly considered the wave steepness, the gradient of slope, the settling velocity of sediment and other factors. The relationship was established between the wave hydrodynamic conditions and the sediment transport, and an empirical formula and a semi-rational formula had been used to estimate the type of the beach profile states.

A large number of experimental studies over the years have greatly improved the present understanding of dynamics within the beach states under wave action. However, there are some disadvantages on the formula of the beach states due to that the situation is so complex. While a set of laboratory experiments were performed on this study, phenomena in a real beach could not be necessarily reproduced in wave flumes. The difference of phenomena in the real beach and laboratory is caused by several factors such as scale effect of physical model, three-dimensional effect of real topographic change, irregularity of real waves, etc. (Mimura et al., 1986).

In this study, we find that the beach states under wave action are related to the above factors, in addition, it is related to the characteristic of breaking waves such as the breaking intensity of plunging waves. Existing methods that have been used to describe wave breaking characteristics employ a non-dimensional parameter, such as the Irribarren number [Eq. (1)] (Irribarren and Nogales, 1949 -cited Mead and Black, 2001), or the surf scaling parameter [Eq. (2)] (Guza and Inman, 1975) and the surf similarity parameter (Battjes, 1974).

$$\xi = i/\sqrt{H_0/L_0}, \tag{1}$$

$$\varepsilon = a_b\omega^2/(gi^2), \tag{2}$$

where, ξ is the Irribarren number, i is a representative beach gradient, H_0 and L_0 are the deepwater waveheight and wavelength, respectively. ε is the surf scaling parameter, a_b is the wave amplitude at breaking, ω is the wave radian frequency and g is the gravity constant.

Longuet-Higgins (1982) proposed fitting the breaking vortex shape of a plunging wave profile to a cubic function, and postulated this may be a better descriptor of the "intensity" of a plunging wave breaking event than the surf similarity parameter (SSP, Fig. 2). The vortex length to width ratio was been identified as a good indicator of the plunging wave breaking intensity, and to enable the breaking intensity of high-quality surfing waves to be clearly communicated, a classification scheme had been created. The breaking wave intensity is described in five categories from extreme to medium (Mead and Black, 2001).

Fig. 2. Cubic vortex fitting to wave shape (Mead and Black, 2001).

where l, w and θ are the vortex length, width and angle in fitting cubic, respectively; H is the estimated wave height.

In this paper, we attempt to analyze the relationship between the state of the sandy beach profile and the characteristics of the plunging wave. Different types of wave in the sandy beach have been considered, and the free surface elevations, the processes of wave propagation, wave breaking, uprush and backwash and the evolution of cross-shore beach profile were measured and recorded, which were used to explore the rule of evolution of the sandy beach profile under wave action. On the basis of experimental results, a concept about the characteristic angle of the plunging wave was put forward through the observation and the analysis of the phenomenon of the laboratory experimental process. A qualitative analysis on the sediment transport by current generated from the plunging wave and the state of beach profile under wave action had been done. The states formula of the sandy beach profile induced by the plunging wave had been established based on the relation of Irribarren number and the state of beach profile. These experimental results and others' experimental results were made use of fitting to three trend lines, and three fitting coefficients were calculated in their formula respectively.

2 Experimental description

2.1 *Experimental setup*

The experiments were carried out in a wave flume equipped with a piston wave generator (Fig. 3), 40 m in length, 0.8 m in depth and 0.5 m in width, equipped with sponge absorption for the control of wave generators in wave flumes. This made it possible for simultaneous generation of desired incident waves, and absorption of the associated reflected waves.

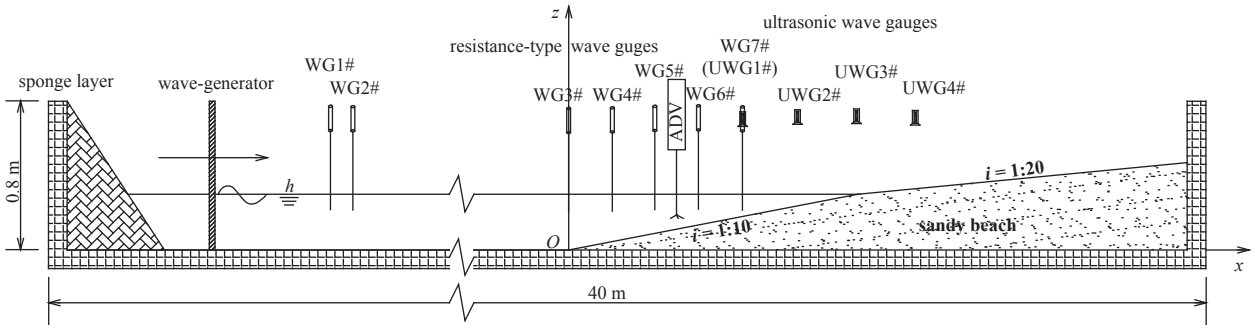

Fig. 3. Schematic diagram of experimental setup. h is the water depth in the wave flume, i the beach gradient.

For the convenience of describing the sand beach and the arrangement of the measuring devices, a flume coordinates system was been noted. The x-axis is aligned with the cross-shore direction, with the positive direction pointing the wave propagation and x=0 defined at the toe of the sandy beach slope. The z direction is aligned in the vertical direction and is positive pointing upward with z=0 defined on the bottom of the basin. The y axis is aligned with the longshore direction. The sensors are numbered sequentially with ascending x or z coordinate.

The laboratory generalization experiment on mechanism of a beach profile evolution had been presented in this study, and the scale setting did not to be considered. The beach (with a combinational slope of 1:10 and 1:20) was formed with 1.81 m^3 (after preliminary sieving) of the natural Xiangjiang River sand. A sieve analysis was performed on the sand samples, and the grain-size distribution obtained from the test is shown in Fig. 4. The grain size were being the mean median diameter d_{50}=0.363 mm, the geometric standard deviation $\sigma_g = \sqrt{d_{84}/d_{16}} = 1.824$, the specific gravity s=2.65, and the fall velocity w=2.39 cm/s. The sand bed thickness was practically nil at the toe while it was 65 cm at the end of the beach, 9.5 m from the toe. Fresh water (from the city tap) was used in the experiments. The nominal water depth is 0.30 m, 0.35 m and 0.40 m with a maximum deviation of ±1 mm. Actual water depths were recorded before each wave.

Three kinds of measurements were made: water surface elevation measurement, fluid velocity measurement and beach profile measurements. Eleven capacitance wave gauges (acquisition at 50 Hz) and non-contact ultrasonic displacement gauges (acquisition at 20 Hz) were used to measure instantaneous water surface elevations, of which seven were resistance-type wave gauges (WG, RBR Inc.) and four were ultrasonic wave gauges

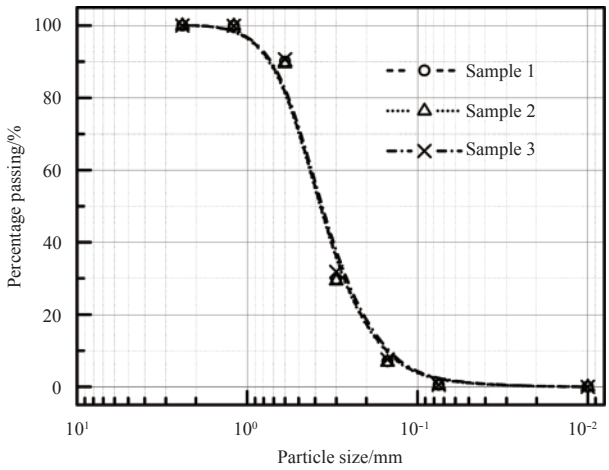

Fig. 4. The grain-size distribution of three samples of the sand used in this experiment.

(UWG, Sinfotek Ltd.). The resistance-type wave gauges were deployed seaward of the shoreline from x=–18.0 m to x=2.5 m and the ultrasonic wave gauges were installed landward of the shoreline, from x=2.5 m to x=4.0 m. Acoustic-Doppler velocimeters (ADV, Nortek Vectrino) were deployed to measure the near-bed fluid velocities on the breaking point. The ADV was kept at approximately 5 cm above the bed by adjusting their vertical positions between the runs. That specific locations were been moved according to the change of experimental condition. The beach profile was measured by the URI-IIIU ultrasonic topographic instrument (UTI, Wuhan University Electronic Information Insti-

tute), which has measurement accuracy up to ±1 mm. Video capture was used to record the whole experiment process. Two cameras (Pro C920 HD Webcam, Logitech Inc.) were located at one side of the wave flume to record the whole experiment process, such as wave uprush and backwash, sediment movement and beach profile changes. The locations of cameras needed to be slightly adjusted for each case.

2.2 *Wave conditions*

The experimental program was divided in two test series (regular wave and cnoidal wave), and within each test series a number of different wave cases were generated (Table 1). Wave conditions were chosen according to the ability of the wave generator and a comparative analysis in different cases and the basis of previous experiments in the wave flume. Typical erosion/accretion threshold criteria based on the relative fall velocity also were being considered, and the final profiles and the net sediment transport are consistent with these initial estimates. In this study, the regular waves and the cnoidal waves were been chosen to impact the sandy beach, which to investigate the evolution rule of the sandy beach profile under wave action.

Table 1. Experimental conditions

Case No.	Wave type	Water depth (h)/m	Wave height (H)/m	Wave period (T)/s	Irribarren number (Eq. (1))	Surf-scaling parameter (Eq. (2))	Waves action time of each stage/min	Number of action stage
1	regular wave	0.30	0.05	1	0.524	2.927	10	3
2	regular wave	0.30	0.09	1	0.391	5.268	3	5
3	regular wave	0.30	0.08	2	0.638	4.682	3	5
4	regular wave	0.35	0.05	1	0.534	2.927	10	3
5	regular wave	0.35	0.12	1	0.345	7.024	3	5
6	regular wave	0.35	0.14	2	0.499	8.194	3	5
7	regular wave	0.40	0.05	1	0.541	2.927	10	3
8	regular wave	0.40	0.14	1	0.323	8.194	3	5
9	regular wave	0.40	0.18	2	0.453	10.536	3	5
10	cnoidal wave	0.30	0.05	2	0.807	2.927	10	3
11	cnoidal wave	0.30	0.12	2	0.521	7.024	3	5
12	cnoidal wave	0.30	0.12	3	0.648	7.024	3	5
13	cnoidal wave	0.35	0.05	2	0.835	2.927	10	3
14	cnoidal wave	0.35	0.14	2	0.499	8.194	3	5
15	cnoidal wave	0.35	0.14	3	0.622	8.194	3	5
16	cnoidal wave	0.40	0.05	2	0.860	2.927	10	3
17	cnoidal wave	0.40	0.17	2	0.466	9.950	3	5
18	cnoidal wave	0.40	0.18	3	0.566	10.536	3	5

Computed Irribarren number [Eq. (1)] (Irribarren and Nogales, 1949 -cited Mead and Black, 2001) ranged between 0.323 and 0.860, and computed surf-scaling parameters [Eq. (2)] (Wright and Short, 1984) ranged between 2.927 and 10.536 (Table 1) during the initial tests for all data sets. Camenen and Larson (2007) graphically analyzed the lines of separation between each breaker type, and postulated that each inflection point in the graph marked a breaker type boundary. According to the wave parameter in this study, the wave breaker category boundaries can be drawn in Fig. 5, and so the types of breaking wave were visually identified as predominantly plunging wave in theory. In fact, the breaking waves that we observed in the experiment were basically the plunging waves.

The circles are experimental results. The lines are breaker type separation lines. The solid line is a nonbreaking boundary and an unstable wave boundary respectively, and dash lines represent a spilling/plunging boundary, plunging/collapsing boundary and a collapsing/surging boundary respectively. The four zones mean that ① a spilling breaker area, ② a plunging breaker area, ③ a collapsing breaker area, ④ a surging breaker area.

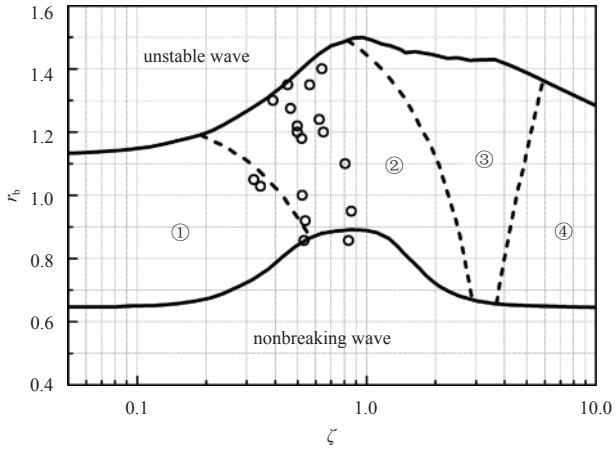

Fig. 5. Breaker type separation (Camenen and Larson, 2007).

2.3 *Summary of the experimental methods*

All the instruments were calibrated according to standard procedures and some repeatability discuss about the experiment were carried out before the tests, including waves generating, initial beach profile manufacturing and beach profile evolution in the same situation. The overall agreement in the experiment was satisfactory following Chen et al. (2012) and Jiang et al. (2015).

Before each test, the flume was first filled slowly with water to the desired water depth, and then the sandy beach was allowed to soak for a long time (more than 12 h). The elevation of the beach profiles was measured by the UTI. The beach profile was measured along two cross-shore sections (y=0.17 and 0.34 m), which the beach profile was all measured twice along each cross-

shore section to minimize possible random measurement errors. For each test condition, the elevation of the beach profile is the average of four measured values.

To research the evolution rule of the beach profile under wave action, the same wave condition was run some stages for each test condition. The time of wave action in each stage and the number of stages in every case are given in Table 1. After each run, the flume was filled slowly with water to a measurement water level to measure the changed beach profile because the UTI can measure only the elevation of an underwater topography. After taking the measurement of the beach profile, the water depth was reduced slowly to the desired experimental water level for the next test run. Typically, a waiting time of about 30 min was allowed before starting a new test run to reduce the possible effects of a residue current in the flume and pore water in the sandy beach. All tests were under this cycling experiment each run.

3 Experimental results and discussion

3.1 *Beach profile elevation change*

As the first topic of the experimental results, a macroscopic beach profile change will be discussed. The cross-shore distributions of the beach profile during the different tests in the experiment when still water depth (h) is 0.35 m are illustrated in Fig. 6. The evolution of the sandy beach profile before and after wave action in different conditions was given in Fig. 6, which included different wave types, different wave heights and different wave periods. They showed each corresponding topography changes in different stage compared with the initial topography.

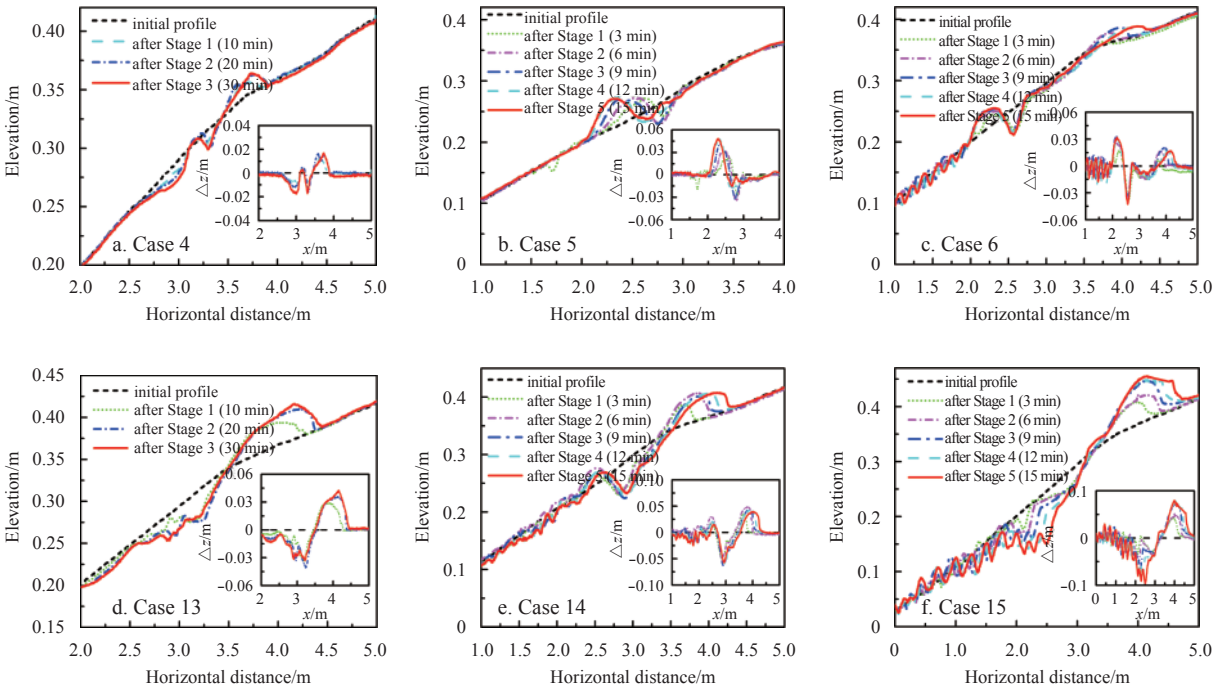

Fig. 6. Experiment results of the beach profiles changes in case: h=0.35 m. a. The regular wave, H=0.05 m, T=1 s; b. the regular wave, H=0.12 m, T=1 s; c. the regular wave, H=0.14 m, T=2 s; d. the cnoidal wave, H=0.05 m, T=2 s; e. the cnoidal wave, H=0.14 m, T=2 s; and f. the cnoidal wave, H=0.14 m, T=3 s.

During Case 4 (Fig. 6a) wave breaking occurred at around x=2.70 m, and two small berms started to be generated around the breaking point under regular wave action, with the crest located at x=3.20 m and 3.70 m. The position of the first beach berm and the two troughs are located in the foreshore area, below the still water surface, while the second beach berm is located in the backshore area, and above the still water surface. In this paper, the first beach berm is defined as the fore-berm, and the second beach berm is defined as post-berm, all the following discuss based on this definition. From the morphology perspective, the width and height of the post-berm are larger than the fore-berm. Two sides of the fore-berm are basic symmetric, then tergal slope of the post-berm is steeper than frontal slope. In this condition, the sandy beach is in the intermediate state form (Wright and Thom, 1977), and the coastline was not erosion nor deposition.

The regular waves (Cases 5 and 6) lead to the coastline erosion and the profile has been called the sand bar in Figs 6b and c. The sediment is transported offshore from the breaking point location, the upper shoreface, and the overall beach slope is reduced. This kind of change can be observed in nature in the case of storm events during which the upper part of the beach is eroded and the profile switches to form a sand bar (Günaydın and Kabdaşlı, 2003b; Grasso et al., 2009). As the experiment proceeding, the berm moves to onshore but the bar moves to offshore. The breaking point of wave moves seaward as the bar evolved, and was usually about 0.4 m offshore of the bar crest. In these two conditions, the sandy beach profiles are bar-trough state, and the coastlines are erosion. The state of beach profile under the regular wave action may appear in different wave types, and affected by the wave height and period.

But as shown in Figs 6d–f, the sandy beach profile under the cnoidal waves action present the berm state. As it evolves, the sediment is transported onshore to the berm, and the slope of sandy beach becomes steeper and the trough is generated around the breaking point. Figures 6e and f show that some sand ripples are development in the offshore zone on sandy beach un-

der the cnoidal wave action in these two sets of experiments. And this phenomenon is somewhat alike to the results of the regular wave (Fig. 6c), but the sand ripples are not significantly generated in those cases of a smaller wave height (Fig. 6d). From the three experimental results, that the sandy beach profile under the cnoidal wave action was obvious change in the first stage can be seen, and changes gradually decrease with the continuous action. This is typical of beach profile reconstruction by fair weather waves following erosion by a strong storm, and its coastline is deposition (Certain and Barusseau, 2005; Grasso et al., 2009).

3.2 *The concept about the characteristic angle of plunging wave*

The experimental results reveal that the profile states of the sandy beach under wave action are concerned with not only wave types but also other related factors like wave height, period, etc. From the single-frame analysis of the high definition videos during the experiments, as shown in Fig. 7, it can be seen that the breaking wave of different type waves on the sediment-bed slope of the beach bed are all plunging wave. Although the types of the breaking waves in these experiments are the plunging waves basically, but the sandy beach profile presents different shapes and states under wave action, which included the sand bar profile and berm profile. As shown in Fig. 7, wave was breaking during propagating from the deep water area to the nearshore area, the water tongue of the plunging wave hit the sandy beach fiercely, which made the sediment to motion conspicuously.

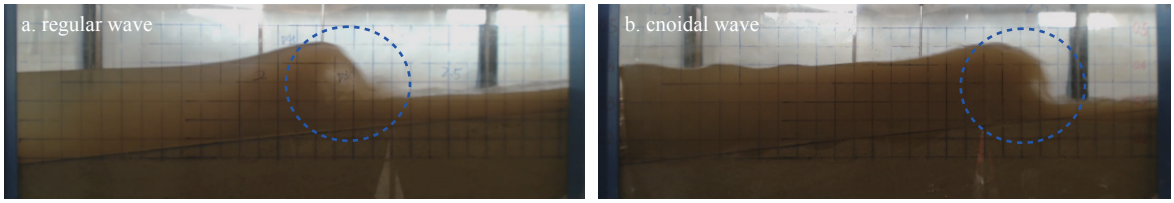

Fig. 7. The breaking wave on the slope.

Two currents that defined as an uprush current and a return current in this paper had been generated from wave water after plunging, as shown in Fig. 8. The return current is offshore movement after plunging, while the uprush current is onshore movement and it will turn to be offshore movement due to backwash. The return current and the uprush current were generated from the plunging wave. When the uprush current run up to the highest point in the slope, it began to fall back in an offshore direction and turn to be a backwash current. Hence, there are three currents near the breaking point. A new local coordinates system taken hit point as the origin of the plunging wave had been noted in Fig. 8. The angle between the water tongue and the slope was defined as the characteristic angle in this paper.

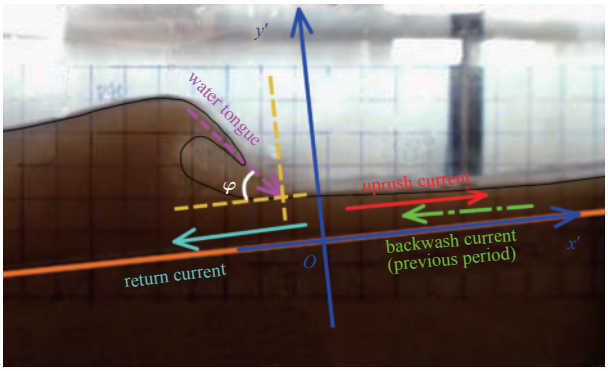

Fig. 8. The schematic of the characteristic angle of the plunging wave.

The sediment carried by the return current, the uprush current and the backwash current would directly state the beach profile states, whose strength is related to such factors as wave elements, slope of beach and so on. As shown in Fig. 8, the intensities of the return current and the uprush current are different because of the different characteristic angle of the plunging wave, while the intensity of the backwash current is different as the different wave period and other factors.

3.3 *Discussion about the characteristic angle*

3.3.1 *Relationship between the angle and the states of beach*

Numerous and high-class researches had been used to investigate and predict the visual geometric differences between the breaking waves. In an effort to quantify the physical differences with the plunging breaker category, Mead and Black (2001) and Robertson and Hall (2013) visually analyzed the laboratory-based regular wave breaking wave profiles and proposed fitting a cubic function to the enclosed vortex in Fig. 2. In this study, the characteristic angle of the plunging wave (Fig. 8) had been used to establish a relationship with the states of the sandy beach.

The bigger of the plunging wave height, the bigger of the characteristic angle correspondingly, which makes the intensity of the return current is strong and the uprush current is rather weak. Sediment near the hit-point of the plunging wave on sandy beach is scouring because of the strong impact action of the plunging wave. The majority of the incipient sediment is transported offshore carried by the return current and accumulated into the sand bar on the offshore side of the sand trough, while small amount of sentiment is transported onshore carried by the uprush current and accumulate into the berm on backshore. The state of the sandy beach is the sandbar profile. On the contrary, the smaller of the plunging wave, the smaller of the characteristic angle correspondingly, which makes the return current weak while the uprush current strong. Therefore, the state of the sandy beach is the berm profile due to that the majority of the incipient sediment is transported onshore carried by the uprush current and accumulate into the berm onshore zone.

In fact, the intensity of these three currents is very difficult to be measure respectively under existing experimental conditions. But we can compare the intensity with onshore current and offshore. If the intensity of onshore current played much more important or dominant roles in the motion process, the sediment would be transported onshore to the berm. And if the intensity of offshore current played much more important or dominant roles in the motion process, the sediment would be transported offshore to the sandbar.

If only with consideration of the current velocity, there are some limitations to discuss about the current intensity and the leading factor. Because maybe one current velocity is very large but in short time, it provides only small influence on the sediment transport. The integral for the current velocity to time have been considered to describe the current intensity in this study. We can compute the integral for the current velocity from the following formula:

$$S = \int_{t_1}^{t_2} v(t)\,\mathrm{d}t. \tag{3}$$

The measured results of velocity in the breaking point of waves in Cases 5 and 13 are shown in Fig. 9. The velocity is greater than 0, indicating that the current is onshore movement, and less than 0, indicating that the current is offshore movement. We can see that S_2 is greater than S_1 in a wave period for Case 5 from Fig. 9a. That means the offshore current plays dominant roles in this condition. The incipient sediment induced by the plunging waves is transported offshore and the sandy beach presented the sand bar profile in Fig. 6b. Figure 9b presents the velocity of current in the breaking point in Case 13, S_1 is greater than S_2 over a period of time in this condition. That means the onshore current plays the dominant roles and the incipient sediment is transported onshore. The sandy beach presented the sand bar profile and the shoreline was advance in Fig. 6d.

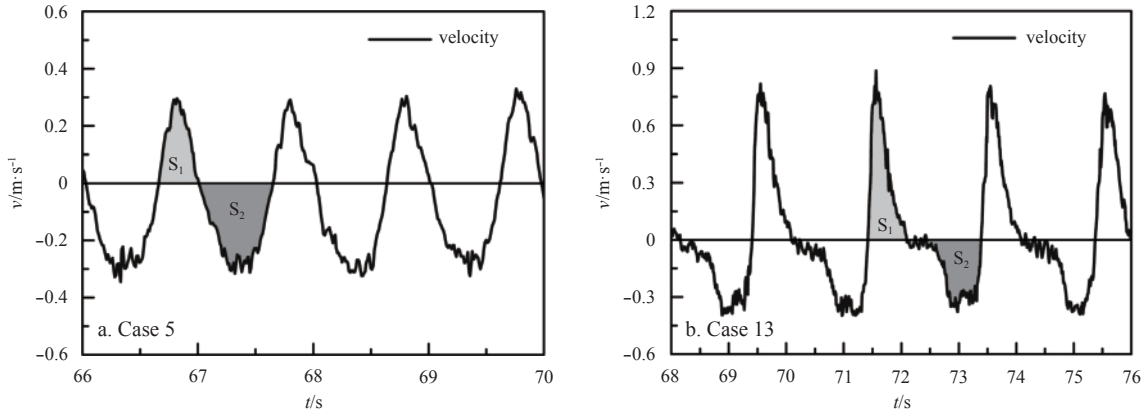

Fig. 9. The velocity of current in the break point of the plunging wave.

The cnoidal wave belongs to the highly nonlinear wave and its wave crest and trough are obviously asymmetric, that is to say, the trough is flat while the crest is pretty steep. Therefore, the energy of cnoidal wave is concentrated on the wave crest. When wave spreads to the slope from deep water, the wave height is larger due to the superimposed impact of the reflected wave, while the wave trough movement would be blocked by the backwash current. Wave crest curls like tongue hit into water and occur to break, which make the characteristic angle small, thus the uprush current is strong while the return current is rather weak. Owing to the intensity of the backwash current is decided by the intensity of the uprush current, and the strong turbulence produced by the meeting of the uprush current and the backwash current. The incipient sediment is transported onshore carried by the uprush current. As the intensity of turbulence and the velocity of uprush current are getting weakened, the incipient sediment is accumulated and the beach profile switches to form the berm state. Meanwhile, the increased impacting range and more concentrated wave energy due to the characteristic angle reduced, the intensity of impact by the plunging wave are getting stronger, thus the erosion range affected by the cnoidal wave is relatively larger than the regular wave.

3.3.2 *Relationship between the characteristic angle and Irribarren number*

The intensity of breaking wave is an important parameter of the states of sandy beach under wave action. The methods used in this study to determine the states of sandy beach are the characteristic angle of the plunging waves. But the angle is not convenient to analyze in the process of actual operation. In order to conduct a quantitative analysis for the relationship between the angle and the states of sandy beach, the relationship between the angle and Irribarren number has been established for the examination of the basic situations of the interaction of beach and plunging waves.

According to Irribarren and Nogales (1949 -cited Mead and Black, 2001), all wave breaking events can be divided into three broad categories depending on the output of Eq. (1), or its breaking equiavalent:

$$\xi_\mathrm{b} = i/\sqrt{H_\mathrm{b}/L_0}. \tag{4}$$

Figure 10 illustrates the relationship between the angle and the Irribarren number. According to the experimental data in the presented paper, the relationship between the characteristic angle of plunging waves and the Irribarren number can be proposed as

$$\xi_\mathrm{b} = -0.247\tan\varphi + 0.864\ 4, \tag{5}$$

where φ is the characteristic angle, and it is measured by a digital image processing technology that is from HD camera. A good relationship between the angle and Irribarren number is found. That is to say, we can use the Irribarren number to reflect the intensity of plunging waves in our experiments.

4 State formula based on Irribarren number

It can be seen from the above that the sandy beach profile under wave action may show different states due to different types of wave, different wave heights and periods, different compositions of sediment and other factors. According to previous re-

search, sediment movement of the sandy beach is a three-dimensional process, but the states of the beach profile are mainly composed by a transverse sediment transport. That is to say, the sediment transport to onshore or offshore affects the states of the sandy beach profile directly. Geographers classify the beach morphology from the geomorphological point at first, which observably raise awareness about the sandy beach profile, but cannot explain the process of the beach profile evolution and rule of sediment movement.

Wave breaking was plunging when it propagated in the sandy beach, and the strong impact from the plunging wave is the mainly dynamics factors of the sediment incipient. The sediment-laden transport by the return current, the uprush current and the backwash current directly determined the profile evolution of the sandy beach, which generated from the plunging wave. In this study, a dimensionless surf similarity parameter was attempted to use as a basic measurement of the intensity for the three currents. Irribarren number had been used for representing dimensionless surf similarity parameter in this paper, and can be calculated according to Eq. (1).

The states of sandy beach under wave action are the result of wave and beach interaction and mutual restriction. The restricting factors include wave factors and beach factors. The wave factors include water depth, wave height, wave period, and the beach factors include sandy slope gradient, density and composition of sediment. So, the state (Φ) of beach profile under wave action can be given in the following equation:

$$\Phi = f(h, H, T, \varphi, i, d, \gamma_s, \gamma_0, \upsilon_e, g), \tag{6}$$

where h is the depth of still water; H and T are the height and period of wave respectively; i is the gradient of the slope; d is the composition of the sediment particle size, replaced by the median particle size (d_{50}) in this paper; γ_s and γ_0 are the unit mass of sediment and water respectively; g is the acceleration of gravity; and υ_e is eddy viscous coefficient. For convenience, Irribarren number is used to replace the characteristic angle (φ) of plunging wave.

Dimensionless has been done for the Eq. (6):

$$\Phi = f\left(\frac{H}{gT^2}, \frac{i}{(H_0/L_0)^{0.5}}, i, \frac{d_{50}}{(gH)^{0.5}T}, \frac{(gH)^{0.5}}{\omega}, \frac{gHT}{\upsilon}\right). \tag{7}$$

According to the dispersion equation of the small amplitude wave theory [Eq. (8)], we can see that gT^2 can reflect the basic characteristics of the wavelength. Hence, $H/(gT^2)$ embodies the physical function of the wave steepness in faculty.

$$L = \frac{gT^2}{2\pi}\tanh kh. \tag{8}$$

In Eq. (7), $(gH)^{0.5}$ has a velocity dimension, therefore $(gH)^{0.5}T$ can be used to represent some characteristics displacement of wave particle under wave action in a period. So, $d_{50}/\left[(gH)^{0.5}T\right]$ can be regarded as the relative grain size of sediment under wave action, and $(gH)^{0.5}/\omega$ can be regarded as the intensity ratio between sediment lifting by waves and sediment deposition, which can reflect the incipient condition. $(gH)^{0.5}/\upsilon$ is the Reynolds number of wave, for determining the wave boundary layer into turbulent state.

The Irribarren number has been added to the equation of energy balance (Bagnold, 1963), and the state formula has been established in Eq. (9) based on this theory.

$$\xi = C' \cdot \frac{(gH)^{0.5}}{\omega}(f_w + i), \tag{9}$$

where C' is a pending dimensionless coefficient; and f_w is the friction coefficient of wave, it can be established which a relationship between the Reynolds number of wave and the relative roughness by using explicit expression [Nielsen, 1992, Eqs (2), (4) and (15)].

$$f_w = \exp\left[5.5(a_m/\Delta)^{-0.2} - 6.3\right], \tag{10}$$

where a_m is displacement amplitude of water particle on the bottom, which can be calculate briefly using small amplitude wave theory in Eq. (11); Δ is equivalent roughness, and can be denoted in a median diameter (d_{50}) in this experimental study.

$$a_m = \frac{H}{2}\frac{1}{\sinh kh}. \tag{11}$$

Equation (9) can be adjusted and to be given by

$$\frac{i}{(H_0/L_0)^{0.5}} = C' \cdot \left[\frac{\gamma_0 gH}{(\gamma_s - \gamma_0)gd_{50}}\right]^{0.5} \times \left\{\exp\left\{5.5\left\{\frac{H_0}{\frac{2\sinh[(2\pi/L_0)h]}{d_{50}}}\right\}^{-0.2} - 6.3\right\} + i\right\}, \tag{12}$$

in this formula, if the left is greater than the right, the sediment would transport to onshore, and the sandy beach profile would present the depositive state. If the left is less than the right, the sediment would transport to offshore, and the sandy beach profile would present the erosive state.

According to Eq. (12), the pending dimensionless coefficient C' of the erosive beach, the depositive beach and the intermediate beach had been obtained respectively by a total of 144 groups of data from these experiments and other experiments in Fig. 11.

$$\left.\begin{array}{ll} \text{For erosive beach} & \dfrac{i}{(H_0/L_0)^{0.5}} < 0.556\ \dfrac{(gH)^{0.5}}{\omega}\ (f_w + i) \\ \text{For depositive beach} & \dfrac{i}{(H_0/L_0)^{0.5}} > 0.556\ \dfrac{(gH)^{0.5}}{\omega}\ (f_w + i) \\ \text{For intermediate beach} & 0.394\ \dfrac{(gH)^{0.5}}{\omega}\ (f_w + i) < \dfrac{i}{(H_0/L_0)^{0.5}} < 0.867\ \dfrac{(gH)^{0.5}}{\omega}\ (f_w + i) \end{array}\right\}. \tag{13}$$

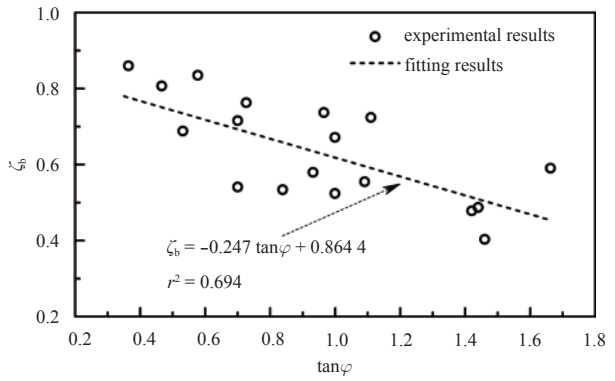

Fig. 10. The relationship between the characteristic angle and Irribarren number.

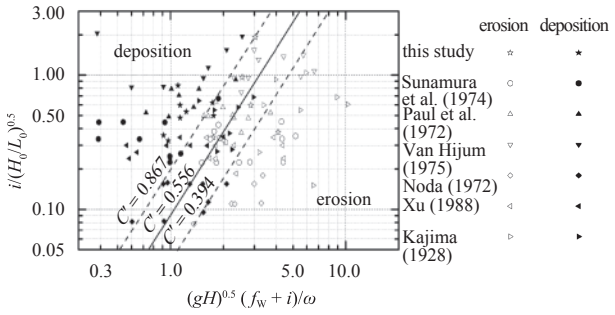

Fig. 11. Distinguishing of the beach profile.

It has been shown that the state of intermediate beach profile is a zonal area in Fig. 11, which indicates that the intermediate beach is a dynamic equilibrium state. Although three states of the sandy beach had been divided clearly in Fig. 11, but there is something to need pointing out, which is that the state formula based on Irribarren number have imperfection because there are still a few discrepant data and all data are come from laboratory but not field. There are scale effects in experimental results, and so the formula coefficient may need to be calculated when the results were applied to the nature coastal engineering.

5 Conclusions

Laboratory experiments were performed to examine the profile evolution rule and profile states of the sandy beach under the plunging wave on a nonuniform sediment-bed slope. The data demonstrate the influence of the regular waves and the cnoidal waves on the profile evolution and the profile states in sandy beach. In this study, 18 different wave conditions were used, encompassing the regular waves and the cnoidal waves. The experiments compare variations in the beach profile evolution and the profile states between two type waves with the same sandy beach and initial still water depth conditions. The sandy beach under the long time wave action had obvious erosion and deposition variation, and the last dynamic equilibrium profile was affected by wave action. In these experimental conditions, the sandy beach under the regular waves showed the sand bar profile and the berm profile. But the sandy beach profile under the cnoidal waves is only the berm profile in this study.

The experimental results show that the profile states of sandy beach under waves action are not only related to the type of waves, but also to other factors, such as wave height, wave period, composition of sediment and gradient of sandy beach slope.

Through the observation and analysis of the phenomenon of the laboratory experimental process, put forward the concept of the characteristic angle of the plunging wave. The qualitative analysis on the sediment transport carried by current generating from the plunging wave and the states of beach profile under wave action had been done. The state formula of the sandy beach induced by plunging wave had been established based on the relation of the Irribarren number and the beach profile. These experimental results and other experimental results were used to fit to the three trend lines, and three formula coefficient is obtained. This formula can divide the sandy beach morphology into the three states clearly, which included deposition beach, erosion beach and intermediate beach.

References

Alsina J M, Cáceres I, Brocchini M, et al. 2012. An experimental study on sediment transport and bed evolution under different swash zone morphological conditions. Coastal Engineering, 68: 31–43

Alsina J M, Falchetti S, Baldock T E. 2009. Measurements and modelling of the advection of suspended sediment in the swash zone by solitary waves. Coastal Engineering, 56(5): 621–631

Bagnold R A. 1940. Beach formation by waves: some model experiments in a wave tank. (includes photographs). Journal of the Institution of Civil Engineers, 15(1): 27–52

Bagnold R A. 1963. Beach and nearshore processes. Part 1: Mechanics of marine sedimentation. The sea, 3(528): 4188–4194

Baldock T E, Alsina J A, Caceres I, et al. 2011. Large-scale experiments on beach profile evolution and surf and swash zone sediment transport induced by long waves, wave groups and random waves. Coastal Engineering, 58(2): 214–227

Baldock T E, Manoonvoravong P, Pham K S. 2010. Sediment transport and beach morphodynamics induced by free long waves, bound long waves and wave groups. Coastal Engineering, 57(10): 898–916

Battjes J A. 1974. Surf similarity, 14th International Conference on Coastal Engineering. Am Soc of Civ Eng, Copenhagen, 466–480

Camenen B, Larson M. 2007. Predictive formulas for breaker depth index and breaker type. Journal of Coastal Research, 23(4): 1028–1041

Certain R, Barusseau J P. 2005. Conceptual modelling of sand bars morphodynamics for a microtidal beach (Sète, France). Bulletin de la Societe Geologique de France, 176(4): 343–354

Chen Jie, Huang Zhenhua, Jiang Changbo, et al. 2012. An experimental study of changes of beach profile and mean grain size caused by tsunami-like waves. Journal of Coastal Research, 28(5): 1303–1312

Dean R G. 1973. Heuristic models of sand transport in the surf zone. In: First Australian Conference on Coastal Engineering: Engineering Dynamics of the Coastal Zone. Australia: Institution of Engineers, 215.

Dean R G. 1991. Equilibrium beach profiles: characteristics and applications. Journal of Coastal Research, 7(1): 53–84

Doering J C, Baryla A J. 2002. An investigation of the velocity field under regular and irregular waves over a sand beach. Coastal Engineering, 44(4): 275–300

Grasso F, Michallet H, Barthélemy E, et al. 2009. Physical modeling of intermediate cross-shore beach morphology: transients and equilibrium states. Journal of Geophysical Research: Oceans (1978–2012), 114(C9): C09001

Günaydın K, Kabdaşlı M S. 2003a. The formation of offshore ripples in the zone under irregular waves. Ocean Engineering, 30(3): 297–307

Günaydın K, Kabdaşlı M S. 2003b. Characteristics of coastal erosion geometry under regular and irregular waves. Ocean Engineering, 30(13): 1579–1593

Guza R T, Inman D L. 1975. Edge waves and beach cusps. Journal of Geophysical Research: Oceans (1978-2012), 80(21): 2997–3012

Hughes M G, Aagaard T, Baldock T E. 2007. Suspended sediment in the swash zone: heuristic analysis of spatial and temporal vari-

ations in concentration. Journal of Coastal Research, 23(6): 1345–1354

Jackson N L, Masselink G, Nordstrom K F. 2004. The role of bore collapse and local shear stresses on the spatial distribution of sediment load in the uprush of an intermediate-state beach. Marine Geology, 203(1): 109–118

Jiang Changbo, Wu Zhiyuan, Chen Jie, et al. 2015. Sorting and sedimentology character of sandy beach under wave action. Procedia Engineering, 116: 771–777

Johnson J W. 1949. Scale effects in hydraulic models involving wave motion. Transactions, American Geophysical Union, 30(4): 517–525

Kajima R, Shimizu T, Maruyama K, et al. 1982. Experiments on beach profile change with a large wave flume. Coastal Engineering: 1385–1404.

Kaneko A. 1985. Formation of beach cusps in a wave tank. Coastal Engineering, 9(1): 81–98

Kobayashi N, Lawrence A R. 2004. Cross-shore sediment transport under breaking solitary waves. Journal of Geophysical Research: Oceans (1978–2012), 109(C3): C03047

Longuet-Higgins M S. 1982. Parametric solutions for breaking waves. Journal of Fluid Mechanics, 121: 403–424

Masselink G, Russell P, Turner I, et al. 2009. Net sediment transport and morphological change in the swash zone of a high-energy sandy beach from swash event to tidal cycle time scales. Marine Geology, 267(1): 18–35

Mead S, Black K. 2001. Predicting the breaking intensity of surfing waves. Journal of Coastal Research, 17 (special issue 29): 51–65

Mimura N, Otsuka Y, Watanabe A. 1987. Laboratory study on two-dimensional beach transformation due to irregular waves. Coastal Engineering 1986: 1393–1406

Nielsen P. 1992. Coastal bottom boundary layers and sediment transport. In: Liu C, Philip LF, eds. Advanced Series on Ocean Engineering. Singapore: World Scientific

Noda E K. 1972. Equilibrium beach profile scale-model relationship. Journal of the Waterways, Harbors and Coastal Engineering Division, 98(4): 511–528

Paul M J, Kamphuis J W, Brebner A. 1973. Similarity of equilibrium beach profiles. Coastal Engineering 1972: 1217–1236

Pritchard D, Hogg A J. 2005. On the transport of suspended sediment by a swash event on a plane beach. Coastal Engineering, 52(1): 1–23

Reniers A, Roelvink D, Dongeren A. 2001. Morphodynamic response to wave group forcing. Coastal Engineering 2000: 3218–3228

Robertson B, Hall K. 2013. Wave Vortex Parameters as an Indicator of Breaking Intensity. Proceedings of World Academy of Science, Engineering and Technology. World Academy of Science, Engineering and Technology (WASET), (73): 576

Roelvink J A, Reniers A J H M. 1995. LIP 11D Delta Flume experiments: a dataset for profile model validation. Report H2130. Netherlands: WL/Delft Hydraulics

Sunamura T, Horikawa K. 1975. Two dimensional beach transformation due to waves. Coastal Engineering 1974: 920–938.

Tzang S Y, Chen Y L, Ou S H. 2011. Experimental investigations on developments of velocity field near above a sandy bed during regular wave-induced fluidized responses. Ocean Engineering, 38(7): 868–877

Van Hijum E. 1975. Equilibrium profiles of coarse material under wave attack.Coastal Engineering 1974: 939–957.

Wright L D, Short A D. 1984. Morphodynamic variability of surf zones and beaches: a synthesis. Marine Geology, 56(1): 93–118

Wright L D, Thom B G. 1977. Coastal depositional landforms: a morphodynamic approach. Progress in Physical Geography, 1(3): 412–459

Xu Xiao. 1988. Types of two-dimension sandy beaches and their criterion. The Ocean Engineering (in Chinese), 6(4): 51–62

Yamaguchi N, Sekiguchi H. 2011. Variability of wave-induced ripple migration in wave-flume experiments and its implications for sediment transport. Coastal Engineering, 58(8): 671–677

Young Y L, Xiao Heng, Maddux T. 2010. Hydro- and morpho-dynamic modeling of breaking solitary waves over a fine sand beach Part I Experimental study. Marine Geology, 269(3–4): 107–118